CHEMISTRY OF MATERIALS



Article

# Head-to-Head Linked Dialkylbifuran-Based Polymer Semiconductors for High-Performance Organic Thin-Film Transistors with Tunable Charge Carrier Polarity

Shengbin Shi, Hang Wang, Mohammad Afsar Uddin, Kun Yang, Mengyao Su, Luca Bianchi, Peng Chen, Xing Cheng, Han Guo, Shiming Zhang, Han Young Woo, and Xugang Guo

*Chem. Mater.*, **Just Accepted Manuscript** • DOI: 10.1021/acs.chemmater.9b00118 • Publication Date (Web): 19 Feb 2019

# Head-to-Head Linked Dialkylbifuran-Based Polymer Semiconductors for High-Performance Organic Thin-Film Transistors with Tunable Charge Carrier Polarity

Shengbin Shi[†, §], Hang Wang[†, ‖, §], Mohammad Afsar Uddin[‡], Kun Yang[†], Mengyao Su[†], Luca Bianchi[†], Peng Chen[†], Xing Cheng[†], Han Guo*[, †], Shiming Zhang[‖], Han Young Woo*[, ‡], Xugang Guo*[,†]

[†] Department of Materials Science and Engineering and The Shenzhen Key Laboratory for Printed Organic Electronics, Southern University of Science and Technology, No. 1088, Xueyuan Road, Shenzhen, Guangdong 518055, China

[‡] Research Institute for Natural Sciences, Department of Chemistry, Korea University, Seoul 02841, South Korea

[‖] Key Laboratory of Flexible Electronics (KLOFE) & Institute of Advanced Materials (IAM), Jiangsu National Synergetic Innovation Center for Advanced Materials (SICAM), Nanjing Tech University, 30 South Puzhu Road, Nanjing, Jiangsu 211816, China

**ABSTRACT**: Planar backbone conformation is essential for enabling polymer semiconductors with high charge carrier mobility in organic thin-film transistors (OTFTs). Benefiting from the smaller van der Waals radius of O atom in furan (versus S atom in thiophene), alkylated furan exerts a reduced steric hindrance on neighboring arene, and it was found that the head-to-head (HH) linked 3,3'-dialkyl-2,2'-bifuran (**BFR)** can attain a high degree of backbone planarity. Hence **BFR** should be a promising building block for constructing polymer semiconductors with planar backbone conformation and hold distinctive advantages over dialkylbithiophene-based analogue, which is typically highly twisted. The alkyl chains on the 3 and 3' positions offer good solubility for the resulting polymers, which in combination with its planar backbone yields an improved molecular design window for developing high-performance polymer semiconductors, particularly those with simple molecular structure and based on the acceptor co-unit without any solubilizing chains. When incorporated into polymer semiconductors, remarkably high hole and electron mobilities of 1.50 and 0.31 $cm^2 V^{-1} s^{-1}$ are obtained from **BFR**-based polymers **FBFR-BO** and **CNBFR-C18** containing fluorinated and cyano-functionalized benzothiadiazole as the acceptor co-unit, respectively. Such mobilities are the highest values for HH linked polymers and also among the best for furan-containing polymers. The results demonstrate that HH linked dialkylbifuran is a highly promising building block for constructing organic and polymeric semiconductors, and this new approach by incorporating HH **BFR** offers several distinctive advantages for developing high-performance polymer semiconductors, including effective optoelectronic property tuning using minimal number of aromatic ring, reduced structural complexity, facile materials synthesis, good materials solubility, and enriching materials library. In addition, the study offers important guidelines for future development of furan-based polymers and head-to-head linkage containing organic semiconductors.

## INTRODUCTION

$\pi$-Conjugated polymers are promising semiconducting materials for the development of next-generation light-weight, flexible, stretchable optoelectronic devices.[1-5] A great amount of research

efforts have been devoted to understanding their chemical structure-materials property-charge transport property correlations, offering important guidelines for new materials design.[6-12] It has been well established that planar backbone conformation with low torsional disorder is highly desirable for polymer semiconductors to facilitate charge transport in both intrachain and interchain regimes.[13-15] Large dihedral angles along polymer backbones not only reduce the $\pi$-conjugation and decrease the electronic coupling between adjacent building blocks, but also hinder the three-dimensional packing of polymer chains and the formation of ordered polymer aggregates, thus limiting intermolecular charge hopping.[16,17] In order to achieve a high degree of backbone planarity, various materials design strategies have been developed and utilized with great successes, including conformation lock via non-covalent intramolecular interactions,[18-21] incorporation of bridged or fused rings,[14,22-24] developing regioregular polymeric backbones,[25] insertion of unsubstituted $\pi$-spacers,[26,27] and heteroatom substitution.[28]

In spite of several promising features demonstrated already, furan, as a thiophene analogue, gained much less attention in the community.[29-32] $\alpha$-Oligofuran is shown to have intrinsically a high backbone planarity with internal dihedral angles close to 0°, while featuring other advantages such as good solubility and reduced environmental impact of being biodegradable and obtainable from renewable resources.[33-35] More importantly, the high degree of backbone planarity in oligofuran and polyfuran appears to persist even with the presence of head-to-head (HH) linkages, benefiting from the small van der Waals radius of the O atom.[36,37] This is in sharp contrast to the scenario associated with 3,3'-dialkyl-2,2'-bithiophene (**BTR**) in which the HH linkage results in a substantial dihedral angle between two thiophene moieties. Therefore, HH linked **BTR** is typically avoided in molecular and polymer semiconductors, and the above mentioned strategies are employed to gain backbone planarity.[20,27,38-42] However, polymer semiconductors built on these strategies often suffer from their own disadvantages, such as elevated energy levels of frontier molecular orbitals (FMOs),[20,39] reduced solubility,[38] or unsatisfactory charge transport properties.[40,41] Since HH linked 3,3'-dialkyl-2,2'-bifuran (**BFR**) can attain planar backbone conformation and the solubilizing chains on the 3 and 3' positions afford the polymer semiconductors with essential solubility,[29,43] therefore **BFR** should be excellent building blocks for constructing polymer semiconductors. The solubilizing alkyl chains on bifuran enable developing polymer semiconductors based on comonomers without any side chains, such as benzothiadiazoles. In addition, the incorporation of **BFR** can yield the resulting polymer with simple structure, featuring minimized number of aromatic ring and reducing synthesis complexity. Such polymers with minimal number of aromatic ring can also result in effectively tuning of the FMO energy levels and enrich the materials library.

In this work, we synthesized a novel HH linked building block **BFR** via a facile synthetic route and performed studies in-depth on the **BFR**-based donor-acceptor (D-A) polymer semiconductors (Figure 1) for the first time. Through comprehensive theoretical studies and experimental characterizations, we systematically investigated the effects of alkyl chains on **BFR** moiety and substituents on the acceptor co-unit on polymer backbone conformation. It was discovered that a planar backbone conformation of **BFR** could be attained in polymers unless both the branched alkyl chain 2-butyloctyl on **BFR** and the bulky cyano substituent on benzothiadiazole are present. When applied in organic thin-film transistors (OTFTs), a remarkable hole mobility ($\mu_h$) of 1.50 $cm^2\ V^{-1}\ s^{-1}$ was achieved from polymer **FBFR-BO,** which is the highest value reported for all HH linked polymers to date, [39-42,44] and also among the best results for furan-containing polymer semiconductors.[28,30,45] By simply changing the acceptor comonomer, the cyano-functionalized polymer **CNBFR-C18** exhibited an electron mobility ($\mu_e$) of 0.31 $cm^2\ V^{-1}\ s^{-1}$, while polymer **CNBFR-BO** with a branched 2-butyloctyl chain on **BFR** showed a much more twisted backbone and less ordered morphology, leading to a substantially lower $\mu_e$ of $9.5 \times 10^{-3}\ cm^2\ V^{-1}\ s^{-1}$. The results demonstrate the versatility of **BFR** for enabling polymer semiconductors to have distinct charge carrier polarity, and the studies show the intrinsic advantages and great potentials of HH linked dialkylbifuran for constructing planar polymer semiconductors with simple structure and facile synthesis, at mean time achieving substantial

charge carrier mobilities in OTFTs.

## RESULTS AND DISCUSSION

***Synthesis of Monomers and Polymer Semiconductors.*** The synthetic route to the distannylated **BFR** monomer **3** is straightforward as depicted in Figure 1a. Starting from 3-bromofuran, compound **1** was readily synthesized by lithiation using lithium diisopropylamide (LDA) followed by the treatment of $CuCl_2$, which was then subjected to Kumada coupling with Grignard reagent alkylmagnesium bromide to afford the HH linked 3,3'-dialkyl-2,2'-bifuran (**2**). In order to achieve sufficient solubility and at the mean time to optimize and study the polymer backbone conformation, chain packing, film morphology, and charge transport property upon side chain variation, both linear *n*-octadecyl (C18) and branched 2-butyloctyl (BO) side chains were attached to the 3 and 3' positions of **BFR**. Next, the distannylated monomers **3a** and **3b** were prepared by conventional lithiation followed by quenching with trimethyltin chloride. The NMR spectra and elemental analysis results indicated a high purity of the distannylated monomers without further purification. The monomers **3a** and **3b** were then copolymerized with brominated difluorobenzothiadiazole (ffBT) or dicyanobenzothiadiazole (DCNBT)[46] comonomer using Stille coupling based polycondensation under microwave irradiation to afford the polymer semiconductors. The NMR spectra of the monomers and polymers were shown in the Supporting Information (Figure S1–S12). The attachment of bifuran to the strong acceptor comonomers is beneficial for the stability of the resulting **BFR**-based polymers, greatly attenuating their decomposition against light and oxygen over time, which is typically observed in $\pi$-conjugated furans.[32,47] After polymerization, the polymers were purified through sequential Soxhlet extraction to remove impurities and low molecular weight fractions. Their number average molecular weights ($M_n$s) were measured by high-temperature gel permeation chromatography (GPC) at 150 °C used 1,2,4-trichlorobenzene as the eluent, showing a moderate $M_n$ between 11.8–19.1 kDa with a polydispersity index (PDI) in the range of 1.2–2.4 (Table 1). The polymers exhibited good solubilities in common organic solvents, such as toluene, chlorobenzene (CB), and 1,2-dichlorobenzene (*o*-DCB). From synthetic points, the solubilizing ability of **BFR** enables the synthesis of polymers containing acceptor co-unit without any side chain, which can enrich materials library. In addition, the polymers feature simple molecular structure without π-space and fused π-system, which can largely reduce synthetic complexity.

It is instructive to compare the solubilities of polymer **FBFR-C18** with its 3,3'-dioctadecyloxy-2,2'-bithiophene based analogue polymer. Using the same *n*-octadecyl chain, the dialkoxybithiophene-based polymer is intractable, while **FBFR-C18** shows sufficient solubility for materials characterization and device fabrication. Such solubility variation reflects the advantages of achieving planar backbone based on the strategy of decreasing steric hindrance by incorporating furan ring versus the strategy of incorporating non-covalent S···O interaction.[29,32,43,48] In addition, dialkoxybithiophene-based polymers typically show high-lying energy levels of the highest occupied molecular orbital levels (HOMOs), which are detrimental to material/device stability, current on/off ratios ($I_{on}/I_{off}$s), and realization of unipolar n-type performance in OTFT devices.

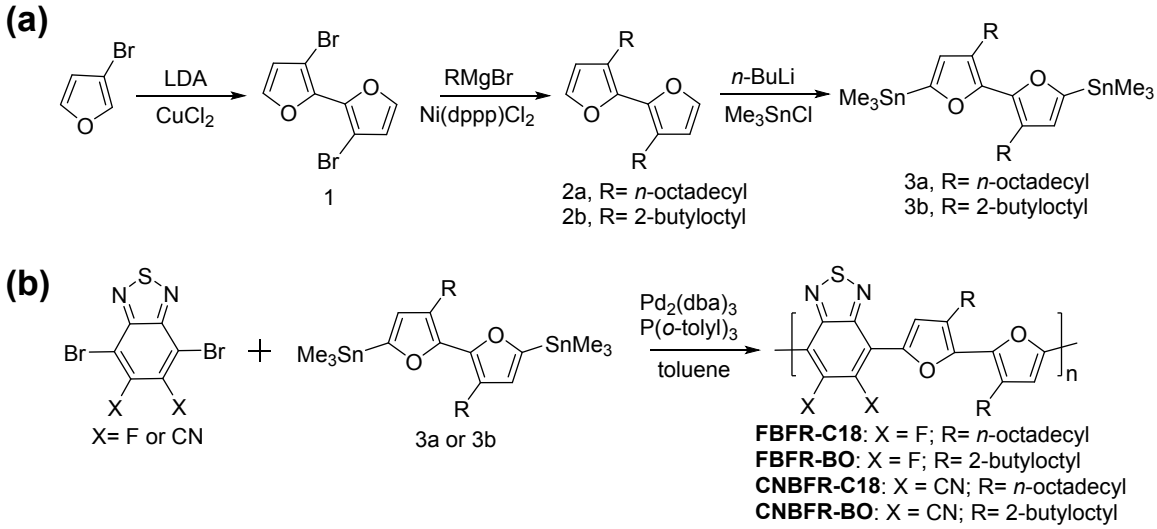


**Figure 1**. Synthetic route to (a) the distannylated head-to-head linked 3,3'-dialkyl-2,2'-bifuran (**BFR**) monomers and (b) the **BFR**-based polymer semiconductors.

**Table 1.** Molecular weights, thermal characteristics, optical absorption, and electrochemical properties of **BFR**-based polymer semiconductors.

| Polymer | $M_n$ [a] [kDa] | PDI [a] | $T_d$ [b] [°C] | $\lambda_{max}$ (soln) [c] [nm] | $\lambda_{max}$ (film) [d] [nm] | $E_{HOMO}$ [e] [eV] | $E_{LUMO}$ [f] [eV] | $E_g^{opt}$ [g] [eV] |
|---|---|---|---|---|---|---|---|---|
| **FBFR-C18** | 19.1 | 2.42 | 401 | 737 | 739 | -5.42 | -3.88 | 1.54 |
| **FBFR-BO** | 13.8 | 1.74 | 394 | 610 | 717 | -5.49 | -3.89 | 1.60 |
| **CNBFR-C18** | 18.9 | 2.04 | 376 | 774 | 906 | -5.65 | -4.41 | 1.24 |
| **CNBFR-BO** | 11.8 | 1.26 | 364 | 756 | 794 | -5.75 | -4.32 | 1.43 |

[a] measured by GPC at 150 °C versus polystyrene standards; [b] decomposition temperature defined as the temperature with a 5% weight loss; [c] from polymer solution ($10^{-5}$ M in *o*-DCB); [d] from thin film on quartz glass; [e] $E_{HOMO} = -(E_{ox}^{onset} + 4.80)$ eV, and $E_{ox}^{onset}$ determined electrochemically using $Fc/Fc^+$ internal standard; [f] $E_{LUMO} = E_{HOMO} + E_g^{opt}$; [g] $E_g^{opt} = 1240/\lambda_{onset}$ eV.

***Thermal and Electrochemical Properties of Polymer Semiconductors.*** Thermogravimetric analysis (TGA) showed that these **BFR**-based polymers have good thermal stability with the decomposition temperature ($T_d$) > 360 °C (Figure S13), defined as the temperature with a 5% weight loss, which allows device optimization over a wide temperature range. Differential scanning calorimetry (DSC) characterization revealed that all these **BFR**-based polymers have distinctive thermal transition (Figure S14), indicative of their high degree of ordering. However, the thermal transition characters are strongly side chain dependent for these polymers. **FBFR-C18** and **CNBFR-C18** showed pronounced melting peaks of side chains centered around 70–80 °C, a phenomenon commonly observed for polymer semiconductors with long linear alkyl chains.[49,50] In contrast, **FBFR-BO** and **CNBFR-BO** with branched 2-butyloctyl chain exhibited primary thermal transition peaks at much higher temperatures of 200 and 176 °C, respectively, as extracted from the cooling processes,

which were likely associated with polymer backbone relaxation.[49] The electrochemical properties of these **BFR**-based polymers are investigated as thin films using cyclic voltammetry (CV, Figure S15) referencing to a ferrocene/ferrocium ($Fc/Fc^+$) internal standard. All polymers show obvious oxidation peaks, and the HOMO energy levels ($E_{HOMO}$s) are derived from oxidation onset, and the data are listed in Table 1. Except **CNBFR-C18**, all other **BFR**-based polymers show weak reduction peaks, hence the lowest unoccupied molecular orbital energy levels ($E_{LUMO}$s) are calculated from the $E_{HOMO}$s and optical band gaps ($E_g^{opt}$s) of polymers (Table 1). The $E_{HOMO}$s and $E_{LUMO}$s are found to be −5.42/−3.88, −5.49/−3.89, −5.65/−4.41, and −5.75/−4.32 eV for **FBFR-C18**, **FBFR-BO**, **CNBFR-C18**, and **CNBFR-BO**, respectively. The branched side chain containing polymers appeared to have slightly deeper $E_{HOMO}$s, associated with their reduced backbone planarity and larger $E_g^{opt}$s seen clearly from the UV-Vis absorption and theoretical study (*vide infra*). By simply changing the substituent from F to CN group on benzothiadiazole, both the HOMO and LUMO energy levels of polymers **CNBFR-C18** and **CNBFR-BO** (versus polymers **FBFR-C18** and **FBFR-BO**) were suppressed by a big margin, particularly the LUMO levels, demonstrating the effective tuning of FMO energy levels. Please note that the FMOs of these **BFR**-based polymers are considerably lower-lying compared to those of their polymers based on alkoxy chain substituted HH bithiophene.[39,51] Although the non-covalent sulfur-oxygen interactions lock the polymer backbone to achieve planar conformation, however the strong electron donating alkoxy chains lead to elevated HOMO levels.[39,46,51] Therefore, our strategy of using dialkylated bifuran shows a distinctive advantage, avoiding high-lying HOMO levels, which should yield improved materials and device stability in OTFTs.[52,53] The narrower $E_g^{opt}$s of the **CNBFR**-based polymers than the **FBFR**-based polymers are mainly attributed to their highly suppressed $E_{LUMO}$s as a result of the strong electron-withdrawing cyano groups.[46] Such deep-positioned $E_{LUMO}$s should facilitate electron injection and promote n-type performance in OTFTs for these **CNBFR**-based polymers (*vide infra*).[53,54]

***Optical Properties of Polymer Semiconductors.*** Optical absorption spectra of these polymers (Figure 2a, 2b) allowed us to gain insights regarding their aggregating properties and conformation changes upon side chain variation on **BFR** and substituent modification on benzothiadiazole moiety. The linear chain substituted **FBFR-C18** exhibited very similar absorption spectra in solution and at film state with an absorption maximum ($\lambda_{max}$) at 737 and 739 nm, respectively, which is attributed to its strong aggregating characteristics with ordered structure in solution (Figure S16). In contrast, the branched 2-butyloctyl substituted **FBFR-BO** is completely disaggregated in solution and undergoes a disorder–order transition when casted into thin-film, yielding a large red-shift of $\lambda_{max}$ from 610 to 717 nm. In comparison to that of **FBFR-BO**, **FBFR-C18** film shows a bathochromic shift of *ca.* 20 nm, which is attributed to the fact that the linear alkyl chain reduces the steric hindrance between two furan rings and hence increases the planarity of polymer backbone. Such structural characters yield strong intermolecular interactions and ordered polymer chains as revealed by X-ray diffraction study (*vide infra*).[30,55] The scenario, in contrast, became quite different for the cyano-functionalized **CNBFR**-based polymers. Both polymers **CNBFR-C18** and **CNBFR-BO** show similar $\lambda_{max}$ at 774 and 756 nm in solution, respectively, implying that the two polymers possess comparable backbone conformation. However, **CNBFR-C18** shows a large bathochromic shift of absorption onset ($\lambda_{onset}$ = 961 nm) compared to **CNBFR-BO** ($\lambda_{onset}$ = 818 nm). Based on the temperature-dependent absorption spectra of the **CNBFR**-based polymer solutions in *o*-DCB (Figure S16), the $\lambda_{onset}$ of **CNBFR-C18** is greatly blue-shifted by 124 nm at 100 °C, indicating that **CNBFR-C18** has a high degree of aggregation in solution at room temperature. However, the temperature increase shows minimal impacts on $\lambda_{max}$ and $\lambda_{onset}$ for polymer **CNBFR-BO**, which indicates that the branched 2-butyloctyl chains on **BFR** greatly suppress the aggregation of polymer **CNBFR-BO** in solution. Such phenomenon is also observed for **FBFR-BO** as the temperature of polymer solution increases. In comparison to polymer solution, the **CNBFR-C18** film displays a large red-shift of $\lambda_{max}$ (132 nm), while the **CNBFR-BO** film shows a much smaller red-shift of $\lambda_{max}$ (38 nm). The results indicate a

substantially different intermolecular aggregation of **CNBFR-C18** and **CNBFR-BO** in solid states.[30,55-57] In fact, **CNBFR-BO** film shows nearly amorphous morphology and lack of diffraction peaks in the X-ray diffraction study (*vide infra*), attributed to a high degree of backbone distortion of polymer **CNBFR-BO** (as revealed by theoretical calculation, *vide infra*), which likely results from steric hindrance between the cyano group on the benzothiadiazole and the neighboring 2-butyloctyl-functionalzied furan. Therefore, both the substituent on benzothiadiazole unit and the side chain on furan moiety are important for polymer backbone conformation, and these **BFR**-based polymers can attain a high degree of backbone planarity unless both the branched alkyl chain on **BFR** and the bulky substituent, i.e. cyano (versus F), on benzothiadiazole, are present.

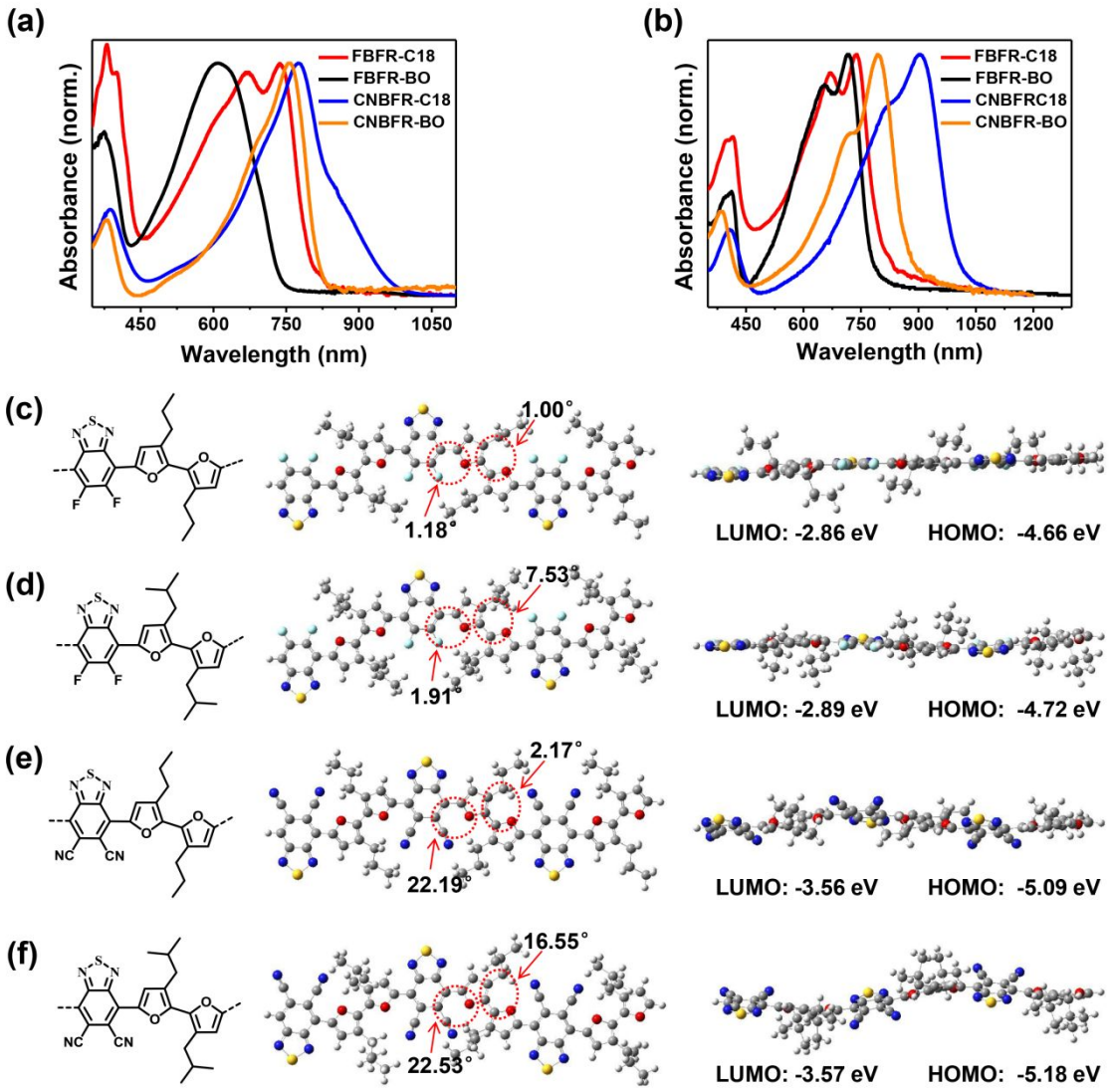


**Figure 2.** UV-vis absorption spectra of the **BFR**-based polymers (a) in diluted *o*-DCB solutions ($10^{-5}$ M) and (b) as thin film spin-casted from *o*-DCB solutions (5 mg $mL^{-1}$). DFT optimized geometries and FMO energy levels of the trimers of the repeat units of (c) **FBFR-C18**, (d) **FBFR-BO**, (e) **CNBFR-C18**, and (f) **CNBFR-BO**. Calculations were carried out at the DFT//B3LYP/6-31G (d, p) level. Dihedral angles between the neighboring arenes are indicated by the red dot circles. The *n*-octadecyl and 2-butyloctyl substituents are replaced by propyl and isobutyl groups, respectively, to simplify the calculations.

**Theoretical Computation of Polymer Semiconductors.** Theoretical computation provides

insights for understanding the backbone conformation of these **BFR**-based polymer semiconductors. Density functional theory (DFT) calculations on the monomer **BFR** only (Figure S17) revealed that linear alkyl chains on the 3 and 3' positions of bifuran do not negatively affect the backbone planarity of HH-linked **BFR** with a dihedral angle of ~0.13°, which was consistent with the earlier report.[32] However, branched alkyl chains show negative effects on backbone planarity, yielding a small dihedral angle of ~8.7° between two furans. Additionally, the torsion potential profiles of both linear and branched alkyl **BFR** were calculated to analyze their thermodynamic stability against torsional disorder. As plotted in Figure S18, the energy minima were located at 0° for **BFR** containing linear alkyl chain and 10° for **BFR** containing branched one, respectively. Metastable state existed at 125° and 130° for **BFR** containing linear and branched alkyl chain, respectively. However, an energy barrier of 3.91 and 3.77 kcal mol$^{-1}$ is needed for the conversion of conformers from their energy minima to the metastable states for **BFR** containing linear and branched alkyl chain, respectively. These results unambiguously suggest that **BFR** containing linear chain favored a more planar conformation and was more stable against torsional disorder compared to **BFR** containing branched one. These findings for the **BFR** units were used as foundation to understand the backbone conformations for the trimers of these polymer repeating units (Figure 2c–2f and Table S1). Polymer **FBFR-C18** exhibited very small dihedral angles not only within the **BFR** units but also between the donor bifuran and acceptor difluorobenzothiadiazole (ffBT) moieties. The high degree of **FBFR-C18** backbone planarity might be assisted by the non-covalent F···H or CH···N interaction between ffBT and **BFR**.[18,42] A high degree of backbone planarity was also found for **FBFR-BO** showing a small dihedral angle of 7.53° within the **BFR** unit, in good accordance with the theoretical computation of single **BFR** (Figure S17). However, polymer **CNBFR-C18** exhibited a large dihedral angle of ~22° between DCNBT and **BFR,** indicating that the bulkier DCNBT acceptor led to an increased steric hindrance compare to ffBT analogue.[46] The backbone of **BFR** in **CNBFR-C18** remained planarity, while it became considerably more twisted with a large dihedral angle of ~16° in **CNBFR-BO** compare to **FBFR-BO**, which hence led to the backbone of polymer **CNBFR-BO** having a high degree of conformation distortion, resulting in the lowest mobility among these **BFR**-based polymers in OTFTs (*vide infra*).

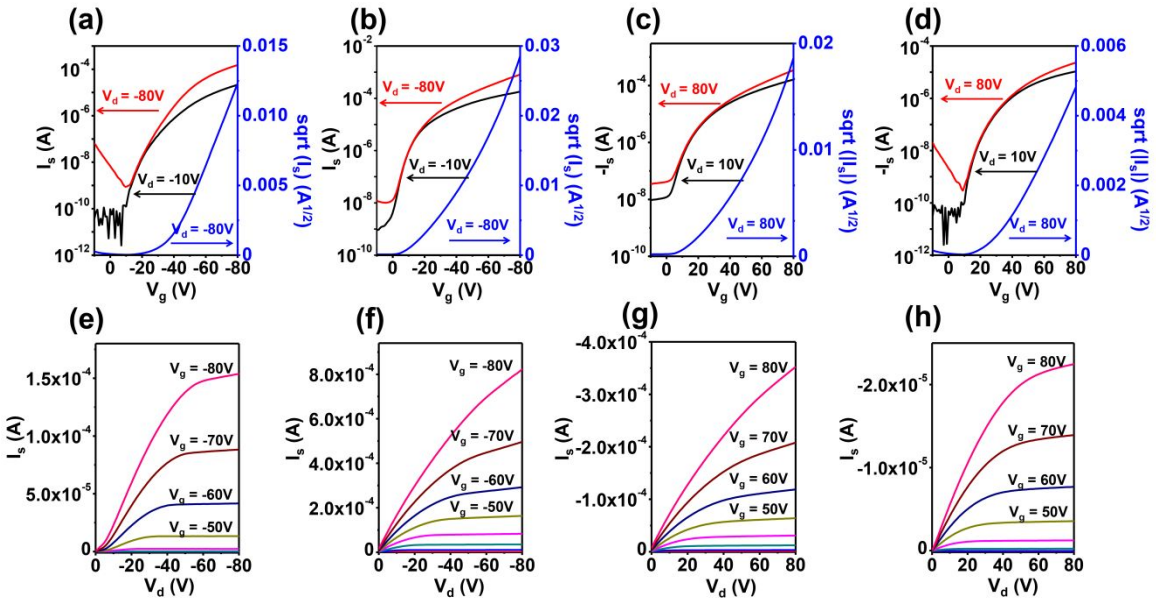


**Figure 3**. Transfer and output characteristics of (a, e) **FBFR-C18**, (b, f) **FBFR-BO**, (c, g) **CNBFR-C18**, and (d, h) **CNBFR-BO**-based OTFT devices fabricated under the optimal conditions. $L$ = 50 μm for **FBFR**-based devices (a, b, e, f) and $L$ = 10 μm for **CNBFR**-based devices (c, d, g, h); $W$ = 5 mm for all transistors.

**Table 2**. TG/BC OTFT device performance parameters using **BFR**-based polymer active layers annealed under the optimal thermal conditions.

| Polymer | Solvent | $T_{anneal}$ | $\mu_h$ [a)] [cm$^2$ V$^{-1}$ s$^{-1}$] | $\mu_e$ [a)] [cm$^2$ V$^{-1}$ s$^{-1}$] | $V_T$ [V] | $I_{on}/I_{off}$ |
|---|---|---|---|---|---|---|
| **FBFR-C18** | *o*-DCB | 160 °C | 0.66 (0.43) | NA | p: -39 | $10^5$ |
| **FBFR-BO** | *o*-DCB | 200 °C | 1.50 (1.10) | NA | p: -26 | $10^4$-$10^5$ |
| **CNBFR-C18** | CF | 200 °C | NA | 0.31 (0.22) | n: 27 | $10^4$ |
| **CNBFR-BO** | CF | 200 °C | NA | $9.5 \times 10^{-3}$ ($7.5 \times 10^{-3}$) | n: 31 | $10^4$-$10^5$ |

[a)] Maximum mobility with an average value shown in parentheses (from at least 5 devices).

**Device Performance of Organic Thin-Film Transistors.** OTFTs with a top-gate/bottom-contact (TG/BC) configuration were subsequently fabricated to investigate the charge transport properties of these **BFR**-based polymers. Figure 3 shows the transfer and output characteristics of the best-performing devices with their performance parameters summarized in Table 2, and the complete set of results under various device fabrication conditions are included in the Supporting Information (Table S2 and S3). It was found that the OTFT performance of these **BFR**-based polymers was sensitive to thermal annealing ($T_{anneal}$), which was generally improved after annealing. **FBFR-C18** and **FBFR-BO** exhibited a maximum $\mu_h$ of only 0.11 and 0.07 cm$^2$ V$^{-1}$ s$^{-1}$ in OTFTs fabricated using the off-center spin-coating (OCSC) technique without thermal treatment, which was significantly enhanced to 0.66 and 1.50 cm$^2$ V$^{-1}$ s$^{-1}$ after annealing at the optimal temperatures of 160 and 200 °C, respectively. The use of OCSC method[58,59] can successfully induce polymer chain alignment across the transistor channel and lead to improved device performance (Table S2), compared to the on-center spin-coated OTFTs fabricated at the same $T_{anneal}$. To the best of our knowledge, this remarkable $\mu_h$ of **FBFR-BO** is the highest reported value for all HH linked polymers,[39-42,44] also among the best results for furan-containing polymers.[28,30,45] Moreover, the off-currents ($I_{off}$s) of $10^{-10}$–$10^{-8}$ A and $I_{on}/I_{off}$s of $10^5$ are much better than those of HH-linked bithiophene-containing analogous polymers with alkoxy side chains, which typically show high $I_{off}$s of $10^{-7}$–$10^{-6}$ A and small $I_{on}/I_{off}$s of $10^2$–$10^3$ in transistors due to the high-positioned FMO energy levels.[46,51,60] The results reflect the advantages of the strategy of reducing steric hindrance by incorporating furan versus the strategy of employing non-covalent S···O interaction by introducing strong electron-donating alkoxy chain. Switching the acceptor monomer to cyano-functionalized benzothiadiazole DCNBT changed the charge carrier polarity to n-type for polymers **CNBFR-C18** and **CNBFR-BO**, as a result of their deep-positioned LUMOs.[46,61] During the device optimization, it was found that the OCSC method unfortunately was ineffective for the **CNBFR**-based polymers because of the chloroform solvent used here. Due to the low boiling point, the film formation time would be too short for the polymer chains to be well aligned in the OCSC films, in view of the much higher spin-casting speed compared to the on-center method. The **CNBFR-C18** OTFTs using on-center spin-casting technique displayed a maximum electron mobility ($\mu_e$) of 0.31 cm$^2$ V$^{-1}$ s$^{-1}$, while it was reduced by more than one order to $9.5 \times 10^{-3}$ cm$^2$ V$^{-1}$ s$^{-1}$ for the **CNBFR-BO** OTFTs. The good device performance of the HH linked **FBFR-BO** and **CNBFR-C18**-based OTFTs is attributed to their appropriately positioned FMO energy level, which should lead to facile charge injection from electrode, as well as the high degree of backbone planarity and good film morphology, including well aligned and interconnected domains, and substantial film crystallinity, which greatly facilitate charge transport. The film morphology will be elaborated below.

It is interesting to note that the low degree of backbone non-planarity is tolerable in polymer semiconductors evidenced by the good OTFT performance of **FBFR-BO** and **CNBFR-C18**. In fact, a small backbone distortion and the presence of dihedral

angle distribution is a general feature for polymer semiconductors, which is the main cause for charge carrier localization along the polymer chain.[15,62] Meanwhile, it is highly important that the disorder in the polymer chain does not interfere with the formation of short-range intermolecular $\pi$-aggregates, that has been recognized as an important factor for efficient charge transport in polymer semiconductors.[7,10] Among the performance parameters achieved by these **BFR**-based polymer semiconductors, the low performance of **CNBFR-BO** was not surprising considering its substantially twisted backbone conformation and near-amorphous film microstructure and morphology (*vide infra*)

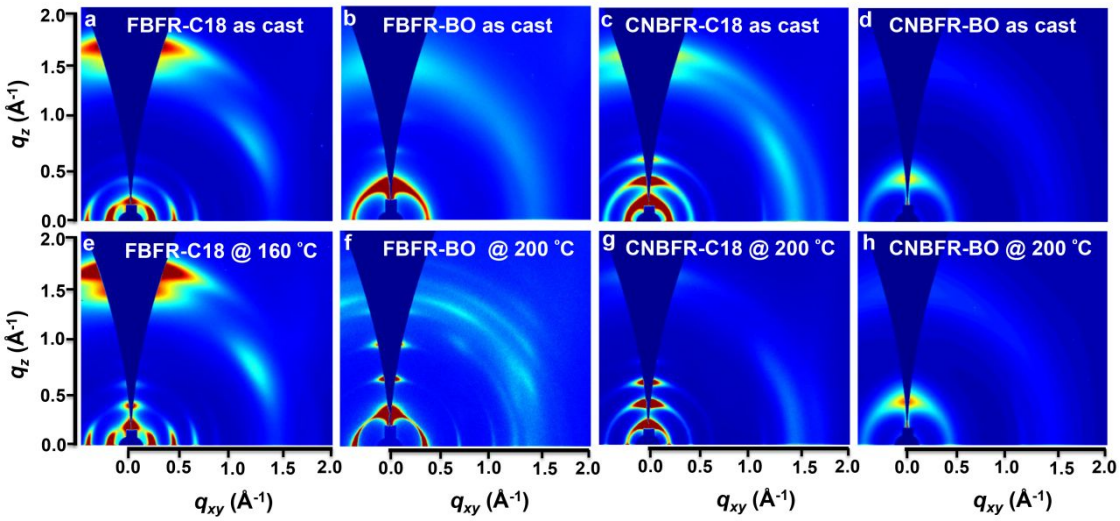


**Figure 4**. 2D-GIWAXS images of the as-cast and thermally annealed films of the **BFR**-based polymers.

***Polymer Film Microstructure and Morphology.*** Film morphology characterizations were carried out using the tapping-mode atomic force microscopy (AFM) and two dimensional grazing incidence wide angle X-ray scattering (2D-GIWAXS) techniques. All **BFR**-based polymer films displayed interconnected nanofibrillar structures in as-cast films (Figure S19). Similar morphological features and surface roughnesses (Table S4) were retained before and after thermal annealing for **FBFR-C18** and **CNBFR-C18**, owing to their high aggregation tendency even in neat film without thermal treatments. With regard to **CNBFR-BO**, thermal annealing induced a negligible change in the AFM surface morphology, as a result of its quite amorphous nature. On the other hand, the thermally treated **FBFR-BO** showed clearly enhanced surface roughness compared to the one without thermal annealing (Table S4), which indicates an effective reorganization of polymer chains by annealing above its thermal transition temperature (see DSC thermograms). The noticeable crystallinity improvement in the AFM morphology explains (in part) the most significantly enhanced OTFT carrier mobility for **FBFR-BO** with thermal annealing.

The detailed interchain packing and orientation of the **BFR**-based polymer films was investigated by 2D-GIWAXS measurements with and without thermal treatments. Figure 4 and S20 present the 2D-GIWAXS images and the corresponding 1D out-of-plane (OOP) and in-plane (IP) line-cut profiles. The resulting packing parameters are summarized in Table S5. Based on the GIWAXS data, the as-cast films of **FBFR-C18** and **FBFR-BO** showed distinctive differences in their packing structures. In the as-cast film without annealing, **FBFR-C18** exhibits strong and well-resolved lamellar scatterings progressing up to (400) with a *d*-spacing of 2.9 nm in the IP direction together with a strong OOP (010) scattering at $q_z$ = 1.80 Å$^{-1}$ with a $d_{\pi-\pi}$-spacing of 0.35 nm, indicating a face-on dominant bimodal orientation. Please note that in addition to the strong OOP (010) scattering at $q_z$ = 1.80 Å$^{-1}$, a much weaker OOP (010) scattering at $q_z$ = 1.55 Å$^{-1}$ was observed, which likely suggest that **FBFR-C18** may have two kinds of π–π stacking spacing of tight (d-spacing of 0.35 nm) and loose (d-spacing of 0.4 nm) cofacial packing. For the polymer with branched chains on bifuran, **FBFR-BO** shows the lamellar peaks progressing up to (300) in the

OOP direction and the IP (100) peak with a $d_{100}$-spacing of 1.8 nm where the smaller lamellar distance of **FBFR-BO** (compared to that of **FBFR-C18**) is due to the short side chain length of 2-butyloctyl. According to the diffraction pattern, polymer FBFR-BO with branched side chain on bifuran shows a dominant edge-on orientation, while polymer FBFR-C18 with linear *n*-octadecyl chain adopts a dominant face-on orientation. Frankly the exact reasons for such different polymer chain orientation are not very clear at this stage. We expect that such orientation variation is related to polymer solubility change by using different side chain, which can alter the polymer aggregating character and hence affect the interaction between the side chain and substrate and the interaction between the polymer backbone and substrate, as well as the competition between these two interactions. The increased film crystallinity and edge-on orientation of polymer chain of **FBFR-BO** (versus **BFR-C18**) is in a good agreement with its higher carrier mobility in OTFT devices.

The as-cast **CNBFR-C18** film with linear *n*-octadecyl side chains shows an edge-on dominant bimodal crystalline ordering where the OOP lamellar scatterings up to (300) are observed with a corresponding lamellar interdigitation distance of ~2.7 nm. In the contrary, the as-cast **CNBFR-BO** film shows an amorphous morphology. This result corroborates the fact that the branched 2-butyloctyl side chains on the **BFR** unit together with the bulky cyano substituents on benzothiadiazole result in a significantly large steric hindrance in the **CNBFR-BO** polymer backbone, inhibiting the crystalline interchain ordering. After thermal annealing, all polymers show a clearly improved film crystallinity confirmed by the sharper and stronger diffraction patterns than the as-cast films, except for **CNBFR-BO** (Figure 4), which still shows a highly amorphous feature. The crystal coherence length (CCL) values based on the IP (100) and OOP (100) peaks were calculated according to the Scherrer equation,[63] showing sharply increased CCL values after thermal treatment (Table S5), which should facilitate the charge carrier transport through intermolecular hopping. Interestingly, thermal treatments noticeably enhanced the edge-on orientation for both **FBFR-BO** and **CNBFR-C18** polymers, as revealed by the intensified lamellar and weakened (010) scattering in the OOP direction. After thermal annealing at 200 °C, **FBFR-BO** shows the most significantly increased CCL of the (100) peak in both IP (105 → 292 Å) and OOP (124 → 218 Å) directions, which together with the enhanced edge-on orientation yields the increased charge carrier mobility measured in OTFT devices.

## CONCLUSIONS

In summary, a novel HH linkage containing building block 3,3'-dialkyl-2,2'-bifuran (**BFR**) was designed and synthesized via a facile synthetic route, and its incorporation into polymers yielded a series of semiconductors with simple molecular structure and tunable charge carrier polarity depending on the acceptor moiety, which reflects the effective polymer optoelectronic property tuning using this BFR building block. We systematically studied the effect of the side chains (*n*-octadecyl or 2-butyloctyl) on bifuran unit and the substituents (fluoro or cyano) on benzothiadiazole moiety on the polymer backbone conformation and its correlation with the absorption spectra, FMO energy levels, film morphologies, and charge transport properties. It was found that the backbone conformation of these **BFR**-based polymers is dependent on the periphery of main chain, and a planar conformation could be attained for the polymer semiconductors unless both the branched 2-butyloctyl chain on **BFR** and the bulky cyano substituent on benzothiadiazole are present. Appropriately positioned FMO energy level, high degree of backbone planarity, ordered polymer chain packing, and hence good OTFT charge transport characteristics were obtained for polymers **FBFR-C18**, **FBFR-BO**, and **CNBFR-C18**. The backbone conformation and chain packing of these **BFR**-based polymers is comparable to that of the alkoxy-functionalized bithiophene-based analogous polymers, but with much lower-lying HOMO energy levels. The results reflect the distinctive advantages of achieving a planar backbone based on the strategy of incorporating furan unit to reduce steric hindrance versus the strategy of incorporating non-covalent S···O interaction. When incorporated into OTFTs, **FBFR-BO** achieved a remarkable $\mu_h$ of 1.50 $cm^2 V^{-1} s^{-1}$, which is the highest value reported for HH linked polymers and among the best results for

furan-containing polymers in OTFTs. The change of the acceptor moiety to cyano-functionalized benzothiadiazole led to polymer **CNBFR-18** with promising n-type performance with a $\mu_e$ of 0.31 $cm^2 V^{-1} s^{-1}$. The results demonstrate that **BFR** is a very promising building block for constructing high mobility polymers with planar backbone conformation. The new approach by incorporating HH linked dialkylbifuran shows several advantages for materials innovation, including effective optoelectronic property tuning, reducing structural complexity using minimal aromatic ring number, facile materials synthesis, and good solubility, which can largely enrich the materials library. Moreover, this detailed study presents a fundamental understanding of the structure-property correlations of **BFR**-based polymers by varying the alkyl chain on bifuran and the substituents on benzothiadiazole, offering important guidelines for future development of HH linked organic semiconductors and furan-based polymers.

## ASSOCIATED CONTENT

### Supporting Information

The Supporting Information material is available free of charge via the Internet at http://pubs.acs.org.

The synthesis and characterization of monomers and polymers, $^1$H and $^{13}$C NMR spectra, thermal, optical, and electrochemical properties of polymers, the DFT calculation, the OTFT fabrication and characterization, and the polymer film morphology.

## AUTHOR INFORMATION


### Corresponding Author

* Han Guo: guoh3@sustc.edu.cn

* Han Young Woo: hywoo@korea.ac.kr

* Xugang Guo: guoxg@sustc.edu.cn


### Author Contributions

§These authors contributed equally.

All authors have given approval to the final version of the manuscript.

### Notes

The authors declare no competing financial interest.

## ACKNOWLEDGMENT

X.G. is thankful for the financial support by the National Science Foundation of China (21774055), Shenzhen Basic Research Fund (JCYJ20170817105905899), Shenzhen Peacock Plan Project (KQTD20140630110339343), the Shenzhen Key Lab funding (ZDSYS201505291525382), and Southern University of Science and Technology (FRG-SUSTC1501A-72). M.A.U. and H.Y.W. are grateful to the financial support from the NRF of Korea (2016M1A2A2940911 and 2015M1A2A2057506).

## REFERENCES


(1) Arias, A. C.; Mackenzie, J. D.; McCulloch, I.; Rivnay, J.; Salleo, A. Materials and Applications for Large Area Electronics: Solution-Based Approaches. *Chem. Rev.* **2010**, *110*, 3-24.

(2) Facchetti, A. π-Conjugated Polymers for Organic Electronics and Photovoltaic Cell Applications. *Chem. Mater.* **2011,** *23*, 733-758.

(3) Yang, J.; Zhao, Z.; Wang, S.; Guo, Y.; Liu, Y. Insight into High-Performance Conjugated Polymers for Organic Field-Effect Transistors. *Chem* **2018**, *4*, 1-38.

(4) Inganäs, O. Organic Photovoltaics over Three Decades. *Adv. Mater.* **2018**, *30*, 1800388.

(5) Wang, S.; Oh, J. Y.; Xu, J.; Tran, H.; Bao, Z. Skin-Inspired Electronics: An Emerging Paradigm. *Acc. Chem. Res.* **2018**, *51*, 1033-1045.

(6) Dong, H.; Fu, X.; Liu, J.; Wang, Z.; Hu, W. 25th anniversary article: key points for high-mobility organic field-effect transistors. *Adv. Mater.* **2013**, *25*, 6158-6183.

(7) Noriega, R.; Rivnay, J.; Vandewal, K.; Koch, F. P.; Stingelin, N.; Smith, P.; Toney, M. F.; Salleo, A. A general relationship between disorder, aggregation and charge transport in conjugated polymers. *Nat. Mater.* **2013**, *12*, 1038-1044.

(8) Olivier, Y.; Niedzialek, D.; Lemaur, V.; Pisula, W.; Müllen, K.; Koldemir, U.; Reynolds, J. R.; Lazzaroni, R.; Cornil, J.; Beljonne, D. 25th Anniversary Article: High-Mobility Hole and Electron Transport Conjugated Polymers: How Structure Defines Function. *Adv. Mater.* **2014**, *26*, 2119-2136.

(9) Sirringhaus, H. 25th Anniversary Article: Organic Field-Effect Transistors: The Path Beyond Amorphous Silicon. *Adv. Mater.* **2014**, *26*, 1319-1335.

(10) Himmelberger, S.; Salleo, A. Engineering semiconducting

polymers for efficient charge transport. *MRS Communications* **2015**, *5*, 383-395.

(11) Son, S. Y.; Kim, Y.; Lee, J.; Lee, G.-Y.; Park, W.-T.; Noh, Y.-Y.; Park, C. E.; Park, T. High-Field-Effect Mobility of Low-Crystallinity Conjugated Polymers with Localized Aggregates. *J. Am. Chem. Soc.* **2016**, *138*, 8096-8103.

(12) Lee, J.; Kang, S.-H.; Lee, S. M.; Lee, K. C.; Yang, H.; Cho, Y.; Han, D.; Li, Y.; Lee, B.; Yang. C. An Ultrahigh Mobility in Isomorphic Fluorobenzo[c]-[1,2,5]thiadiazole-Based Polymers. *Angew. Chem. Int. Ed.* **2018**, *57*, 13629-13634.

(13) Prins, P.; Grozema, F. C.; Schins, J. M.; Patil, S.; Scherf, U.; Siebbeles, L. D. A. High Intrachain Hole Mobility on Molecular Wires of Ladder-Type Poly(*p*-Phenylenes). *Phys. Rev. Lett.* **2006**, *96*, 146601.

(14) Holliday, S.; Donaghey, J. E.; McCulloch, I. Advances in Charge Carrier Mobilities of Semiconducting Polymers Used in Organic Transistors. *Chem. Mater.* **2013**, *26*, 647-663.

(15) Venkateshvaran, D.; Nikolka, M.; Sadhanala, A.; Lemaur, V.; Zelazny, M.; Kepa, M.; Hurhangee, M.; Kronemeijer, A. J.; Pecunia, V.; Nasrallah, I.; Romanov, I.; Broch, K.; McCulloch, I.; Emin, D.; Olivier, Y.; Cornil, J.; Beljonne, D.; Sirringhaus, H. Approaching disorder-free transport in high-mobility conjugated polymers. *Nature* **2014**, *515*, 384-388.

(16) Troisi, A.; Shaw, A. Very Large $\pi$-Conjugation Despite Strong Nonplanarity: A Path for Designing New Semiconducting Polymers. *J. Phys. Chem. Lett.* **2016**, *7*, 4689-4694.

(17) Wang, Y.; Guo, H.; Harbuzaru, A.; Uddin, M. A.; Arrechea-Marcos, I.; Ling, S.; Yu, J.; Tang, Y.; Sun, H.; López Navarrete, J. T.; Ortiz, R. P.; Woo, H. Y.; Guo, X. (Semi)ladder-Type Bithiophene Imide-Based All-Acceptor Semiconductors: Synthesis, Structure-Property Correlations, and Unipolar n-Type Transistor Performance. *J. Am. Chem. Soc.* **2018**, *140*, 6095-6108.

(18) Jackson, N. E.; Savoie, B. M.; Kohlstedt, K. L.; Olvera de la Cruz, M.; Schatz, G. C.; Chen, L. X.; Ratner, M. A. Controlling Conformations of Conjugated Polymers and Small Molecules: The Role of Nonbonding Interactions. *J. Am. Chem. Soc.* **2013**, *135*, 10475-10483.

(19) Huang, H.; Yang, L.; Facchetti, A.; Marks, T. J. Organic and Polymeric Semiconductors Enhanced by Noncovalent Conformational Locks. *Chem. Rev.* **2017**, *117*, 10291-10318.

(20) Guo, X.; Kim, F. S.; Jenekhe, S. A.; Watson, M. D. Phthalimide-Based Polymers for High Performance Organic Thin-Film Transistors. *J. Am. Chem. Soc.* **2009**, *131*, 7206-7207.

(21) Kim, F. S.; Guo, X.; Watson, M. D.; Jenekhe, S. A. High-Mobility Ambipolar Transistors and High-Gain Inverters from a Donor-Acceptor Copolymer Semiconductor. *Adv. Mater.* **2010**, *22*, 478-782.

(22) McCulloch, I.; Ashraf, R. S.; Biniek, L.; Bronstein, H.; Combe, C.; Donaghey, J. E.; James, D. I.; Nielsen, C. B.; Schroeder, B. C.; Zhang, W. Design of Semiconducting Indacenodithiophene Polymers for High Performance Transistors and Solar Cells. *Acc. Chem. Res.* **2012**, *45*, 714-722.

(23) Osaka, I.; Abe, T.; Shinamura, S.; Takimiya, K. Impact of Isomeric Structures on Transistor Performances in Naphthodithiophene Semiconducting Polymers. *J. Am. Chem. Soc.* **2011**, *133*, 6852-6860.

(24) Chen, J.; Yang, K.; Zhou, X.; Guo, X. Ladder-Type Heteroarene-Based Organic Semiconductors. *Chem. Asian. J.* **2018**, *13*, 2587-2600.

(25) Ying, L.; Huang, F.; Bazan, G. C. Regioregular narrow-bandgap-conjugated polymers for plastic electronics. *Nat. Commun.* **2017,** *8*, 14047.

(26) Fei, Z.; Pattanasattayavong, P.; Han, Y.; Schroeder, B. C.; Yan, F.; Kline, R. J.; Anthopoulos, T. D.; Heeney, M. Influence of Side-Chain Regiochemistry on the Transistor Performance of High-Mobility, All-Donor Polymers. *J. Am. Chem. Soc.* **2014**, *136*, 15154-15157.

(27) Osaka, I.; Mccullough, R. D. Advances in Molecular Design and Synthesis of Regioregular Polythiophenes. *Acc. Chem. Res.* **2008**, 41, 1202-1214.

(28) Matsidik, R.; Luzio, A.; Askin, Ö.; Fazzi, D.; Sepe, A.; Steiner, U.; Komber, H.; Caironi, M.; Sommer, M. Highly Planarized Naphthalene Diimide-Bifuran Copolymers with Unexpected Charge Transport Performance. *Chem. Mater.* **2017**, *29*, 5473-5483.

(29) Gidron, O.; Bendikov, M. *α*-Oligofurans: An Emerging Class of Conjugated Oligomers for Organic Electronics. *Angew. Chem. Int. Ed.* **2014**, *53*, 2546-2555.

(30) Chen, M. S.; Lee, O. P.; Niskala, J. R.; Yiu, A. T.; Tassone, C. J.; Schmidt, K.; Beaujuge, P. M.; Onishi, S. S.; Toney, M. F.; Zettl, A.; Frechet, J. M. Enhanced Solid-State Order and Field-Effect Hole Mobility through Control of Nanoscale Polymer Aggregation. *J. Am. Chem. Soc.* **2013**, *135*, 19229-19236.

(31) Xiong, Y.; Tao, J.; Wang, R.; Qiao, X.; Yang, X.; Wang, D.; Wu, H.; Li, H. A Furan-Thiophene-Based Quinoidal Compound: A New Class of Solution-Processable High-Performance n-Type Organic Semiconductor. *Adv. Mater.* **2016**, *28*, 5949-5953.

(32) Cao, H.; Rupar, P. A. Recent Advances in Conjugated Furans. *Chem. Eur. J.* **2017**, *23*, 14670-14675.

(33) Gidron, O.; Diskin.-Posner, Y.; Bendikov, M. *a*-Oligofuran. *J. Am. Chem. Soc.* **2010**, *132*, 2148-2150.

(34) Bunz, U. H. *a*-Oligofurans: molecules without a twist. *Angew. Chem. Int. Ed.* **2010**, *49*, 5037-5040.

(35) Binder, J. B.; Raines, R. T. Simple Chemical Transformation of Lignocellulosic Biomass into Furans for Fuels and Chemicals. *J. Am. Chem. Soc.* **2009**, *13*1, 1979-1985.

(36) Jin, X. H.; Sheberla, D.; Shimon, L. J.; Bendikov, M. Highly Coplanar Very Long Oligo(alkylfuran)s: A Conjugated System with Specific Head-to-Head Defect. *J. Am. Chem. Soc.* **2014**, *136*, 2592-2601.

(37) Qiu, Y.; Fortney, A.; Tsai, C.-H.; Baker, M. A.; Gil, R. R.; Kowalewski, T.; Noonan, K. J. T. Synthesis of Polyfuran and Thiophene-Furan Alternating Copolymers Using Catalyst-Transfer Polycondensation. *ACS Macro Lett.* **2016**, *5*, 332-336.

(38) McCulloch, I.; Heeney, M.; Bailey, C.; Genevicius, K.; Macdonald, I.; Shkunov, M.; Sparrowe, D.; Tierney, S.; Wagner, R.; Zhang, W.; Chabinyc, M. L.; Kline, R. J.; McGehee, M. D.; Toney, M. F. Liquid-crystalline semiconducting polymers with high charge-carrier mobility. *Nat. Mater.* **2006**, *5*, 328-333.

(39) Shi, S.; Liao, Q.; Tang, Y.; Guo, H.; Zhou, X.; Wang, Y.; Yang, T.; Liang, Y.; Cheng, X.; Liu, F.; Guo, X. Head-to-Head Linkage Containing Bithiophene-Based Polymeric Semiconductors for Highly Efficient Polymer Solar Cells. *Adv. Mater.* **2016**, *28*, 9969-9977.

(40) Wang, Y.; Liao, Q.; Wang, G.; Guo, H.; Zhang, X.; Uddin, M. A.; Shi, S.; Su, H.; Dai, J.; Cheng, X.; Facchetti, A.; Marks, T. J.; Guo, X. Alkynyl-Functionalized Head-to-Head Linkage Containing Bithiophene as a Weak Donor Unit for High-Performance Polymer Semiconductors. *Chem. Mater.* **2017**, *29*, 4109-4121.

(41) Vegiraju, S.; Chang, B.-C.; Priyanka, P.; Huang, D.-Y.; Wu, K.-Y.; Li, L.-H.; Chang, W.-C.; Lai, Y.-Y.; Hong, S.-H.; Yu, B.-C.; Wang, C.-L.; Chang, W.-J.; Liu, C.-L.; Chen, M.-C.; Facchetti. A. Intramolecular Locked Dithioalkylbithiophene-Based Semiconductors for High-Performance Organic Field-Effect Transistors. *Adv. Mater.* **2017**, *29*, 1702414.

(42) Liao, Q.; Wang, Y.; Uddin, M. A.; Chen, J.; Guo, H.; Shi, S.; Wang, Y.; Woo, H. Y.; Guo, X. Drastic Effects of Fluorination on Backbone Conformation of Head-to-Head Bithiophene-Based Polymer Semiconductors. *ACS Macro Lett.* **2018**, 7, 519-524.

(43) Gidron, O.; Varsano, N.; Shimon, L. J.; Leitus, G.; Bendikov, M. Study of a bifuran vs. bithiophene unit for the rational design of *π*-conjugated systems. What have we learned? *Chem. Commun.* **2013**, *49*, 6256-6258.

(44) Guo, X.; Liao, Q.; Manley, E. F.; Wu, Z.; Wang, Y.; Wang, W.; Yang, T.; Shin, Y.-E.; Cheng, X.; Liang, Y.; Chen, L. X.; Baeg, K.-J.; Marks, T. J.; Guo, X. Materials Design via Optimized Intramolecular Noncovalent Interactions for High-Performance Organic Semiconductors. *Chem. Mater.* **2016**, *28*, 2449-2460.

(45) Luzio, A.; Fazzi, D.; Nübling, F.; Matsidik, R.; Straub, A.; Komber, H.; Giussani, E.; Watkins, S. E.; Barbatti, M.; Thiel, W.; Gann, E.; Thomsen, L.; McNeill, C. R.; Caironi, M.; Sommer, M. Structure–Function Relationships of High-Electron Mobility Naphthalene Diimide Copolymers Prepared Via Direct Arylation. *Chem. Mater.* **2014**, *26*, 6233-6240.

(46) Shi, S.; Wang, H.; Chen, P.; Uddin, M. A.; Wang, Y.; Tang, Y.; Guo, H.; Cheng, X.; Zhang, S.; Woo, H. Y.; Guo, X. Cyano-substituted benzochalcogenadiazole-based polymer semiconductors for balanced ambipolar organic thin-film transistors. *Polym. Chem.* **2018**, *9*, 3873-3884.

(47) Wang, X.; Chen, S.; Sun, Y.; Zhang, M.; Li, Y.; Li, X.; Wang, H. A furan-bridged D-π-A copolymer with deep HOMO level: synthesis and application in polymer solar cells. *Polym. Chem.* **2011**, *2*, 2872-2877.

(48) Jeffries-EL, M.; Kobilka, B. M.; Hale, B. J. Optimizing the Performance of Conjugated Polymers in Organic Photovoltaic Cells by Traversing Group 16. *Macromolecules* **2014,** *47*, 7253-7271.

(49) Osaka, I.; Zhang, R.; Sauvé, G.; Smilgies, D.-M.; Kowalewski, T.; McCullough, R. D. High-Lamellar Ordering and Amorphous-Like *π*-Network in Short-Chain Thiazolothiazole-Thiophene Copolymers Lead toHigh Mobilities. J. Am. Chem. Soc. **2009**, 131, 2521-2529.

(50) Yang, C.; Orfino, F. P.; Holdcroft, S. A Phenomenological Model for Predicting Thermochromism of Regioregular and Nonregioregular Poly(3-alkylthiophenes). *Macromolecules* **1996**, *29*, 6510-6517.

(51) Chen, J.; Yan, Z.; Tang, L.; Uddin, M. A.; Yu, J.; Zhou, X.; Yang, K.; Tang, Y.; Shin, T. J.; Woo, H. Y.; Guo, X. 1,4-Di(3-alkoxy-2-thienyl)-2,5-difluorophenylene: A Building Block Enabling High-Performance Polymer Semiconductors with Increased Open-Circuit Voltages. *Macromolecules* **2018,** *51*, 5352-5363.

(52) Kim, D. H.; Lee, B.-L.; Moon, H.; Kang, H. M.; Jeong, E. J. Park, J.-Ⅱ.; Han, K.-M.; Lee, S.; Yoo, B. W.; Koo, B. W.; Kim, J. Y.; Lee, W. H.; Cho, K.; Becerril, H. A.; Bao, Z. Liquid-Crystalline Semiconducting Copolymers with Intramolecular Donor–Acceptor Building Blocks for High-Stability Polymer Transistors. *J. Am. Chem. Soc.* **2009**, *131*, 6124-6132.

(53) Zhao, Y.; Guo, Y.; Liu, Y. 25th Anniversary Article: Recent Advances in n-Type and Ambipolar Organic Field-Effect Transistors. *Adv Mater* **2013,** *25*, 5372-5391.

(54) Anthony, J. E.; Facchetti, A.; Heeney, M.; Marder, S. R.; Zhan, X. n-Type Organic Semiconductors in Organic Electronics. *Adv. Mater.* **2010**, *22*, 3876-3892.

(55) Mao, H.; Xu, B.; Holdcroft, S. Synthesis and Structure-Property Relationships of Regioirregular Poly(3-hexylthiophenes). *Macromolecules* **1993**, *26*, 1163-1169.

(56) Liu, D.; Yang, L.; Wu, Y.; Wang, X.; Zeng, Y.; Han, G.; Yao, H.; Li, S.; Zhang, S.; Zhang, Y.; Yi, Y.; He, C.; Ma, W.; Hou, J. Tunable Electron Donating and Accepting Properties Achieved by Modulating the Steric Hindrance of Side Chains in A-D-A Small-Molecule Photovoltaic Materials. *Chem. Mater.* **2018,** *30*, 619-628.

(57) Ostroverkhova, O.; Shcherbyna, S.; Cooke, D. G.; Egerton, R. F.; Hegmann, F. A.; Tykwinski, R. R.; Parkin, S. R.; Anthony, J. E. Optical and transient photoconductive properties of pentacene and functionalized pentacene thin films: Dependence on film morphology. *J. Appl. Phys.* **2005,** *98*, 033701.

(58) Yuan, Y.; Giri, G.; Ayzner, A. L.; Zoombelt, A. P.; Mannsfeld, S. C.; Chen, J.; Nordlund, D.; Toney, M. F.; Huang, J.; Bao, Z. Ultra-high mobility transparent organic thin film transistors grown by an off-centre spin-coating method. *Nat. Commun.* **2014**, *5*, 3005.

(59) Kim, N.-K.; Jang, S.-Y.; Pace, G.; Caironi, M.; Park, W.-T.; Khim, D.; Kim, J.; Kim, D.-Y.; Noh, Y.-Y. High-Performance Organic Field-Effect Transistors with Directionally Aligned Conjugated Polymer Film Deposited from Pre-Aggregated Solution. *Chem. Mater.* **2015**, *27*, 8345-8353.

(60) Huang, J.; Guo, H.; Uddin, M. A.; Yu, J.; Woo, H. Y.; Guo, X. Fluorinated Head-to-Head Dialkoxybithiophene: A New Electron-Donating Building Block for High-Performance Polymer Semiconductors. *Adv. Electron. Mater.* **018**, *4*, 1700519.

(61) Casey, A.; Han, Y.; Fei, Z.; White, A. J. P.; Anthopoulos, T. D.; Heeney, M. Cyano substituted benzothiadiazole: a novel acceptor inducing n-type behaviour in conjugated polymers. *J. Mater. Chem. C.* **2015**, *3*, 265-275.

(62) Jackson, N. E.; Kohlstedt, K. L.; Savoie, B. M.; Olvera de la Cruz, M.; Schatz, G. C.; Chen, L. X.; Ratner, M. A. Conformational Order in Aggregates of Conjugated Polymers. *J. Am. Chem. Soc.* **2015**, *137*, 6254-6262.

(63) Smilgies, D.-M. Scherrer grain-size analysis adapted to grazing-incidence scattering with area detectors. *J. Appl. Cryst.* **2009,** *42*, 1030-1034.

## ToC Graphic